THE SZEWALSKI INSTITUTE OF FLUID-FLOW MACHINERY
POLISH ACADEMY OF SCIENCES

TRANSACTIONS OF THE INSTITUTE OF FLUID-FLOW MACHINERY

116

WYDAWNICTWO IMP PAN

GDAŃSK 2005

TRANSACTIONS OF THE INSTITUTE OF FLUID-FLOW MACHINERY
Appears since 1960

Aims and Scope

Transactions of the Institute of Fluid-Flow Machinery have primarily been established to publish papers from four disciplines represented at the Institute of Fluid-Flow Machinery of Polish Academy of Sciences, such as:

- Liquid flows in hydraulic machinery including exploitation problems,
- Gas and liquid flows with heat transport, particularly two-phase flows,
- Various aspects of development of plasma and laser engineering,
- Solid mechanics, machine mechanics including exploitation problems.

The periodical, where originally were published papers describing the research conducted at the Institute, has now appeared to be the place for publication of works by authors both from Poland and abroad. A traditional scope of topics has been preserved.

Only original and written in English works are published, which represent both theoretical and applied sciences. All papers are reviewed by two independent referees.

EDITORIAL AND PUBLISHING OFFICE

IFFM Publishers (Wydawnictwo IMP), The Szewalski Institute of Fluid Flow Machinery, Fiszera 14, 80-952 Gdańsk, Poland, Tel.: +48(58)3411271 ext. 141, Fax: +48(58)3416144, E-mail: esli@imp.gda.pl http://www.imp.gda.pl/

Terms of subscription

Subscription order and payment should be directly sent to the Publishing Office

Warunki prenumeraty w Polsce

Wydawnictwo ukazuje się przeciętnie dwa lub trzy razy w roku. Cena numeru wynosi 20,- zł + 5,- zł koszty wysyłki. Zamówienia z określeniem okresu prenumeraty, nazwiskiem i adresem odbiorcy należy kierować bezpośrednio do Wydawcy (Wydawnictwo IMP, Instytut Maszyn Przepływowych PAN, ul. Gen. Fiszera 14, 80-952 Gdańsk). Osiągalne są również wydania poprzednie. Prenumerata jest również realizowana przez jednostki kolportażowe RUCH S.A. właściwe dla miejsca zamieszkania lub siedziby prenumeratora. W takim przypadku dostawa następuje w uzgodniony sposób.

Articles in *Transactions of the Institute of Fluid-Flow Machinery* are abstracted and indexed within:

INSPEC Database;
Energy Citations Database;
Applied Mechanics Reviews;
Abstract Journal of the All-Russian Inst. of Sci. and Tech. Inf. VINITI.

ISSN 0079-3205

TRANSACTIONS OF THE INSTITUTE OF FLUID-FLOW MACHINERY

No. 116, 2004, 3-26

V. TSYIMBALYUK,[a] A. ZINKOWSKIJ[a] and ROMUALD RZĄDKOWSKI[b*]

Experimental investigation of palisade flutter for the harmonic oscillations

[a] *Institute for Problems of Strength of the National Academy of Sciences of Ukraine, Timirjazivska St. 2, 01014 Kyiv, Ukraine*

[b] *The Szewalski Institute of Fluid-Flow Machinery, Polish Academy of Sciences, Fiszera 14, 80-952 Gdańsk, Poland*

Abstract

The experimental stand for the flutter analysis was described. In this stand one can measure simultaneously unsteady aerodynamic force and moment with arbitrary combinations of bending and torsion motions of airfoil cascades in the subsonic flow. The cascade is composed of nine blades, four of them are vibrating. Unsteady flow effects have been investigated for subsonic flow in a compressor cascade. Specifically, experimental forced bending and torsion vibration were performed. The aerodynamic work coefficient of bending and torsional cascade vibrations for different interblade phase angles, Strouhal Numbers, and the incidence angles were shown.

Keywords: Palisade flutter; Inviscid flow

Nomenclature

AIC	–	aerodynamic influence coefficients
b	–	chord of airfoil model
B_i	–	induction
i_{ci}	–	current supplied to the moving i-th coil
i	–	incidence flow angle
F	–	force
F_0	–	force developed by the pair of vibrators in the case of vibrations without a flow
h	–	length of airfoil model;
I	–	moment of inertia relative to the axis of rotating
IBPA	–	interblade phase angle

*Corresponding author. E-mail address: z3@imp.gda.pl

K_y, K_α	–	stiffness coefficients of the elastic elements
K_A	–	drag force
l_{ci}	–	length of the ith conductor of the coil
L	–	lift force
$[l]$	–	aerodynamic influence coefficients
M_s	–	moment
M_0	–	moment developed by the pair of vibrators in the case of vibrations without a flow
m	–	mass of the suspension with the vane
$[m]$	–	aerodynamic influence coefficients
M_1	–	inlet Mach number
q_y, q_α	–	coefficient of mechanical resistance in the corresponding directions
$\mathrm{Sh} = (b \cdot 2\pi\nu)/\upsilon_2$	–	reduced frequency
x_m	–	coordinate of center of mass
y_α	–	amplitude of the vibrations
t/b	–	pitch-to-chord ratio
V	–	velocity of incident flow
W	–	aerodynamic work coefficient
ω	–	natural frequency
φ_k	–	phase shift between the k-th force and the current of the vibrator
ψ_k	–	phase shift between the vibrator current and the displacement of the elastic suspension
ρ	–	density of incident flow, b and h are chord and length of airfoil model
α_k	–	angle between chord and tangent to midline of airfoil tip
α_0	–	vibration amplitude
β_1	–	inflow angle
γ	–	stagger angle

1 Introduction

Cases of flutter-type instability are sometime encountered in the course of developing new gas turbine engines. Costly testing is necessary to eliminate this problem. One of the main problems in predicting flutter at the engine design stage is determining the transient aerodynamic loads that develop during the vibrations of blades. This problem is particularly important in the case of separated flow, when theoretical methods of determining the transient aerodynamic loads are not yet sufficiently reliable. Thus, in this study, we use an experimental method of determination of the transient aerodynamic loads on the vibrating blades of turbine engine.

The aeroelastic results of bending vibrations of 2D linear cascade in subsonic flow were published in [1, 2], and torsional [3]. The experimental results of aero-damping and dynamic stability of compressor cascades under bending-torsional vibrations were presented in [4]. Useful benchmark data for unsteady cascade flows, can be found in [5] for the EPFL series of Standard configurations. The complexity of determination of critical conditions of self-induced vibrations (flutter) initiation is concerned with difficulty of measurement of unsteady loads (moments and forces) that act on blades vibrating in the gas flow.

Aerodynamic loads are measured indirectly either through the aerodynamic damping of blade vibrations [11, 12] or the distribution of transient pressures on the blade surfaces [13, 14]. They are measured directly with an extensometric dynamometer [15, 16] or on the basis of the forces developed by vibrators [16, 17]. However, the experimental methods [11-17] allow measurement of the aerodynamic force L and/or the moment M only in the presence of bending or torsion displacements – a situation that does not always reflect the actual modes of vibration of the blades.

In the Institute for Problems of Strength of NAS of Ukraine the appropriate 2D experimental bench was developed that allows us to measure simultaneously unsteady aerodynamic force and moment with arbitrary combinations of bending and torsion motions of airfoil cascades in the subsonic flow. Description of such test bench is given in paper [18].

2 Test stand

To realize flow about the compressor vane cascade with prescribed velocities and angles of attack, the cascade was placed in a wind tunnel (Fig. 1) in which Mach numbers up to 0.7 could be attained. The four central vanes in the cascade were secured to individual vibration units and could undergo prescribed vibrations with two degrees of freedom. Since there was some mechanical coupling even with vibration-proofing elements between the units, it was necessary to keep the vibrations in all of the units steady (whether there was a flow or not) in order to prevent this coupling from affecting the measurement results. Proceeding on the basis of this requirement, we employed an eight-channel feedback system to automatically control the vibrations of the vanes (vibration units). The system also controls the voltages and, thus, the forces on the vibrator coils so as to reduce the difference between the signal of the master oscillator and the vane vibration signal obtained in each channel (the equipment used was described in more detail in [17]). The individual airfoils vibration unit (Fig. 2) has two elastic elements of different widths. The auxiliary (narrow) elastic element does not impede the twisting of the main (wide) element about its own longitudinal axis, and during flexural vibrations the two elements form an elastic parallelogram. This setup ensures constant vibration parameters along the vane. The unit just described also makes it possible to change the natural frequencies of the suspension by using replaceable main elements differing only in thickness.

To improve vibration-proofing the suspension is mounted on another oscillatory system with the same degree of freedom but much greater mass (Fig. 3). The second system includes the permanent magnets of vibrators and ballast. The

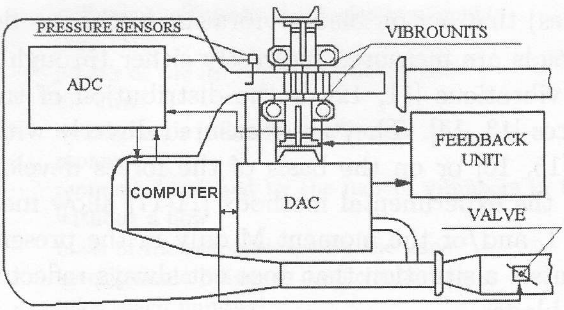

Figure 1. Test stand

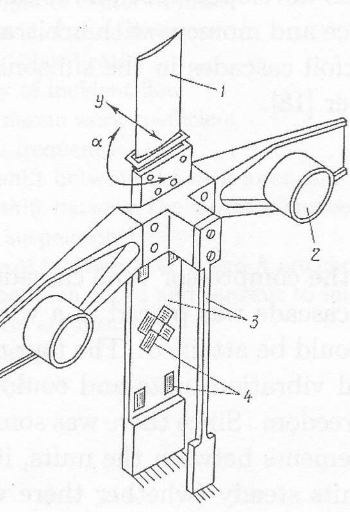

Figure 2. The individual airfoils vibration units: 1 – blade, 2 – moving coil of vibrator, 3 – elastic element, 4 – strain gauges.

second oscillatory system has natural frequencies an order lower than the working system.

The vane is made of carbon-fiber-reinforced plastic, which increases its natural frequency. The other airfoils of the cascade are fixed on rotating disks of active section of the wind tunnel (Fig. 4). The rotation of the disks allows changing incidence angle of the cascade airfoils. For effective control of airflow periodicity adjustable walls and rotating screens of the outlet channel are used. The walls are tuned for cascade airfoils. Since the periodicity of airflow basically depends on right tuning of the angle of airflow outlet from the cascade, thus for reliable control of this angle it is necessary that rotating wall (see Fig. 4) has the length as fifteen times as great as the airfoil chord. Drag outlets of inter-blade channels are joined

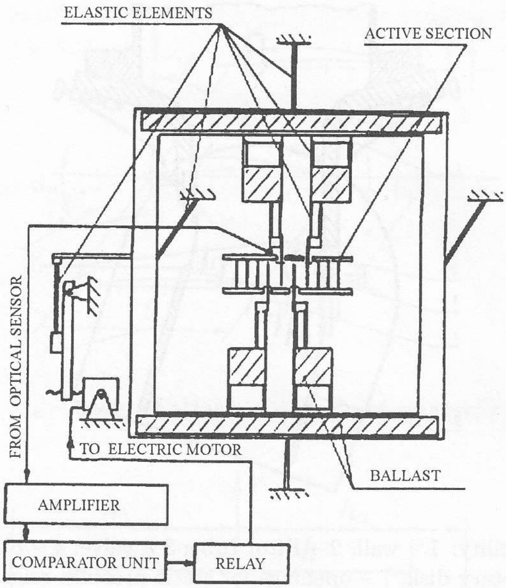

Figure 3. Vibration units

with electrical differential manometers. The criterion of attainment of airflow periodicity in the cascade is the equality of static pressures in corresponding points of inter-airfoil channels.

3 Measurement of transient aerodynamic forces and moments

Since the direction of the aerodynamic forces and moments being measured coincides with the directions of the displacement y and α (see Fig. 5), electrodynamic vibrators can be used to excite the vibrations and measure the loads. The force developed by such a vibrator can be determined in accordance with Ampere's law from the current i_{ci} supplied to the moving ith coil:

$$F_i = B_i l_{ci} i_{ci} \quad (i = 1, 2), \tag{1}$$

where l_{ci} is the length of the i-th conductor of the coil, located in a magnetic field with induction B_i.

Figure 6 shows the scheme devised for the elastic suspension of a vane having two degrees of freedom. Aerodynamic loads develop during flow about a vane secured by the yoke shown in Fig. 6, and the equations describing the vibrations of the suspension under the influence of the force and moment developed by the

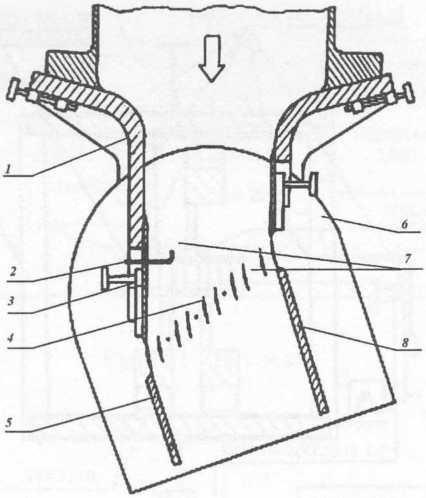

Figure 4. Linear test facility: 1 – wall; 2 – Pitot tube; 3 – valve; 4 – blade; 5, 8 – outlet rotary screens; 6 – rotary disk; 7 – openings for static pressure release

pair of vibrators

$$F_s = F_1 + F_2, \quad M_s = h(F_1 - F_2) \tag{2}$$

can be written in the form

$$\begin{cases} m\ddot{y} + q_y\dot{y} + K_y y + mx_M\ddot{\alpha} = L + F_s\,, \\ I\ddot{\alpha} + q_a\dot{\alpha} + K_\alpha \alpha + mx_M\ddot{y} = M + M_s\,, \end{cases} \tag{3}$$

where m is the mass of the suspension with the vane; I is the moment of inertia relative to the axis of rotation; x_m is the coordinate of center of mass; K_y, K_α are the stiffness coefficients of the elastic elements: q_y, q_α are the coefficients of mechanical resistance in the corresponding directions.

In the case of the absence of flow, $L = 0$, $M = 0$. If the vibrations of the suspension are kept constant in this case

$$\begin{cases} m\ddot{y} + q_y\dot{y} + K_y y + mx_M\ddot{\alpha} = F_0\,, \\ I\ddot{\alpha} + q_a\dot{\alpha} + K_\alpha \alpha + mx_M\ddot{y} = M_0\,. \end{cases} \tag{4}$$

F_0 and M_0 are the force and moment developed by the pair of vibrators in the case of vibrations without a flow), then the left sides of (3) are cancelled by substraction of the corresponding equations (4). In this case the aerodynamic loads

$$L = F_0 - F_s, \quad M = M_0 - M_s\,. \tag{5}$$

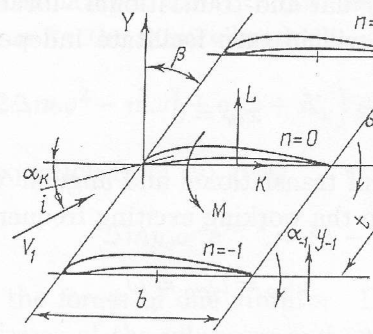

Figure 5. Vane cascade: α_k – angle of attack; β – angle of stagger; t – pitch of cascade; b – chord of vane.

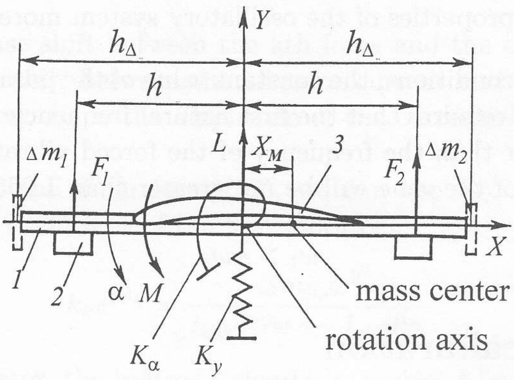

Figure 6. Elastic suspension of a vane: 1 – yoke; 2 – moving coil of vibrator; 3 – test vane; F_1, F_2 – forces from the vibrators, K_y, K_α – flexural and torsional rigidities; Δm_1, Δm_2 – calibrating masses. The arrows denote the positive directions of the aerodynamic loads and the displacement of the vane.

The linear aerodynamic forces and the moment corresponding to linear loads in the section of the blading ring being modeled are obtained after division of L and M by the length of the vane.

Thus, to determine the aerodynamic forces and moments, it is necessary to measure the currents in the moving coils of the vibrators in the presence and absence of flow while keeping the prescribed vibrations of the vanes unchanged.

To reduce the error of the determination of the aerodynamic loads from the difference in two measurements and to improve the sensitivity of the measuring instrument, it is necessary to reduce F_0 and M_0. This can be done under the following conditions:

1. The center of mass of the elastic suspension must coincide with the axis

of rotation (here, the angular and translational vibrations will be mechanically uncoupled, which will in turn facilitate independent control of the vibrations:

$$x_m = 0\,. \tag{6}$$

2. The natural frequencies of translational and angular vibrations of the suspension must be equal to the working exciting frequency:

$$\omega_{yo} = \omega_{\alpha o} = \omega\,. \tag{7}$$

3. Mechanical damping must be negligible, for this to be true, the masses of the vibrating parts of the suspension should be small and the number of joints in the suspension should be minimal. Realization of the last condition will make the properties of the oscillatory system more stable.

In addition to these conditions, the constant value of the parameters of the vibrations along the vane requires that the first natural frequency of the vane must be several times greater than the frequency of the forced vibrations. For example, the dynamic factor of the vane will be not greater than 1.065 at

$$\omega_1 > 4\omega. \tag{8}$$

4 Dynamic calibration

Experience has shown that when the frequency of the alternating current increases, the proportionality factor between the current and the force of the vibrator is no longer equal to Bl_c and instead becomes a complex quantity due to a phase shift between the force and the current. Dynamic calibration at the prescribed frequency is necessary to determine the value of this coefficient. As the known harmonic loads, it is possible to use the inertial force and moment that develop during harmonic vibration from known additional masses Δm_1 and Δm_2 fastened to the yoke (Fig. 6).

The calibration is simplified if we satisfy condition (6) by making the elastic suspension symmetric relative to the Y axis and excite translational vibrations. Then in the absence of flow the forces developed by the pair of vibrations will be the same and the moment will be equal to zero. The equation of the forces acting during harmonic vibrations of the suspension takes the form

$$\left(-m\omega^2 + q_y\omega + K_y\right) y_a e^{j\omega\, t} = 2F_0\,, \tag{9}$$

where y_α is the amplitude of the vibrations, j is the imaginary unit.

If calibrating masses $\Delta m_1 = \Delta m_2 = \Delta m$ are attached to the yoke of the elastic suspension, then for the same vibrations.

$$\left(-2\Delta m\omega^2 - m\omega^2 + q_y\omega + K_y\right) y_a e^{j\omega\, t} = 2F\,. \tag{10}$$

Substraction of this equation from (9) gives

$$-\Delta m y_a \omega^2 e^{j\omega\, t} = F_0 - F\,, \tag{11}$$

where F_0 and F are the forces of one vibrator. During harmonic vibrations of the suspension, the forces of the vibrators and currents in the moving coil will also be harmonic. For example, for the kth ($k = 1, 2$) vibrator

$$F_k = k_k e^{j\varphi_k} i_{ck} = k_k e^{j\varphi_k} I_{ck} e^{j(\omega\, t + \psi_k)}\,, \tag{12}$$

where φ_k is the phase shift between the kth force and the current of the vibrator, ψ_k is the phase shift between the vibrator current and the displacement of the elastic suspension, I_{ck} is the amplitude of the current, k_k is the calibration coefficient.

Representing F_0 and F in form (12), we can use Eq. (11) to obtain the complex calibration coefficient of the first vibrator

$$k_k e^{j\varphi_k} = \frac{\Delta m y_s \omega^2}{I_{c0k} e^{j\psi_{0k}\cdot} - I_{ck} e^{j\psi_k}}\,. \tag{13}$$

For the second vibrator, the indices 1 should be replaced by 2.

5 Aerodynamic characteristics

Cylindrical sections of the blade are modelled by the plane airfoil cascade (Fig. 5). For more accurate determination of the aerodynamic load per unit length, the airfoil cascade placed in a wind tunnel must have flow parameters, geometric characteristics and vibration parameters constant along the airfoil. In this case, it is assumed that airfoil aerodynamic loads per unit length of airfoils and of the blade sections being modelled are equal.

Different modes of the blade assembly vibration correspond to different combinations of the translations (x, y) and angular (α) displacements of airfoils, and aerodynamic loads, which occur on them, can be presented in the form of forces L_A, K_A and moment M_A. Method for determination of these aerodynamic loads was developed under assumption of realisation of the following conditions:

- the displacement of the blades in the x direction is negligible; therefore the drag force K_A can be neglected [12],

- the influence of the vibration of only adjacent airfoils from each side on considered airfoil is taken into account.

The selection of these conditions for aerodynamic loads determination suggests the following:

- The airfoil is modelled as a system with two degrees of freedom.
- The influence of a maximum of five airfoils on overall aerodynamic load of considered airfoil cascade is taken into account. These airfoils are called determinative airfoils later on in this paper.
- When the vibration amplitudes on airfoils are small, the first harmonic of aerodynamic force L_A and moment M_A are linearly dependent on these vibrations and are determined from the expressions:

$$L_A = \frac{\rho V^2 bh}{2}\,[l]\,\{q\}\,, \qquad M_A = \frac{\rho V^2 b^2 h}{2}\,[m]\,\{q\} \tag{14}$$

where ρ and V are density and velocity of incident flow, b and h are chord and length of airfoil model;

$$\{q\} = \begin{pmatrix} \dots \\ \bar{y}_n \\ \alpha_n \\ \dots \end{pmatrix} \tag{15}$$

is the column-vector of specified combination of airfoils complex displacements, which account for phase shift both between their displacements and between translation and angular components of this displacements;

$$\bar{y}_n = y_n/b;$$

is the non-dimensional displacement, n is number of determinative airfoil;

$$\begin{aligned} [l] &= [\dots, l_{ny}, l_{n\alpha}, \dots]\,; \\ [m] &= [\dots, m_{ny}, m_{n\alpha}, \dots]\,, \end{aligned} \tag{16}$$

are row-vectors of the aerodynamic influence coefficients (AIC), which represent complex coefficients of proportionality between displacement y or α of n-th airfoil and the induced aerodynamic force or moment on initial airfoil.

In accordance with aforementioned conditions analytical expressions are presented for the case of five determinative airfoils, i.e. $n = -2, -1, 0, 1, 2$. Every airfoil has two degrees of freedom, so all input square matrices and column-vectors (rows) are of 10^{th} order.

The aerodynamic loads on initial or zero ($n = 0$) airfoil are determined as a sum of forces and moments induced by individual components of the displacements of considered and adjacent to it airfoils:

$$
\begin{aligned}
L_A &= \frac{\rho V^2 bh}{2} \sum_{n=-2}^{2} (l_{ny}\bar{y}_n + l_{n\alpha}\alpha_n);\\
M_A &= \frac{\rho V^2 b^2 h}{2} \sum_{n=-2}^{2} (m_{ny}\bar{y}_n + m_{n\alpha}\alpha_n).
\end{aligned}
\tag{17}
$$

The row-vectors of AIC $[l]$ and $[m]$, are determined on the basis of results of experimental measurement of first harmonics of aerodynamic loads L_A and M_A under 10 linear independent combination of airfoil displacements y and α. Thus, in accordance with the number of determinate AIC, we can get two matrix linear equations dependent on unknown AIC:

$$
\begin{aligned}
[L_A^{ex}] &= \frac{\rho V^2 bh}{2} [l] \cdot [q^{ex}];\\
[M_A^{ex}] &= \frac{\rho V^2 b^2 h}{2} [m] \cdot [q^{ex}],
\end{aligned}
\tag{18}
$$

where $[q^{ex}]$ is the displacements square matrix, obtained from column-vectors (15) for the selected displacements combinations; $[L_A^{ex}]$, $[M_A^{ex}]$ are the row-vectors of experimentally defined first harmonics of aerodynamic loads L_A andM_A for the selected displacements combinations. From Eqs. (18) one could derive expressions for column-vectors of AIC:

$$
\begin{aligned}
[l] &= \frac{2}{\rho V^2 bh} [L_A^{ex}] \cdot [q^{ex}]^{-1};\\
[m] &= \frac{2}{\rho V^2 b^2 h} [M_A^{ex}] \cdot [q^{ex}]^{-1}.
\end{aligned}
\tag{19}
$$

Taking into account one component of displacement of considered airfoil in the experiment, the displacement matrix $[q^{ex}]$ becomes diagonal

$$
[q^{ex}] = \begin{pmatrix} \bar{y}_{-2} & 0 & .0.. & 0 \\ 0 & \alpha_{-2} & 0... & 0 \\ & \cdots\cdots\cdots & & \\ 0 & ... & 0...0 & \alpha_2 \end{pmatrix}, \tag{20}
$$

as a result, every matrix equation (19) breaks into independent equations with one unknown variable and AIC could be defined by the expressions:

$$\begin{aligned} l_{ny} &= \frac{2L_{ny}}{\rho V^2 bh \cdot \bar{y}_n}; \\ l_{n\alpha} &= \frac{2L_{n\alpha}}{\rho V^2 bh \cdot \alpha_n}; \\ m_{ny} &= \frac{2M_{ny}}{\rho V^2 b^2 h \cdot \bar{y}_n}; \\ m_{n\alpha} &= \frac{2M_{n\alpha}}{\rho V^2 b^2 h \cdot \alpha_n}, \\ n &= -2; -1; 0; 1; 2. \end{aligned} \tag{21}$$

It is worth mentioning, that in the experiment, in spite of only one component of the displacement of one airfoil to be set at a time, the matrix $[q^{ex}]$ is not strictly diagonal. Therefore, AIC were defined with the equations (18). If column-vectors of AIC $[l]$ and $[m]$ are known, the aerodynamic loads for selected flow regime could be computed for various combinations of translations and angular displacements of airfoils.

The translation harmonic displacements of airfoils can be expressed as

$$\bar{y}_n = |\bar{y}_0|\, e^{j(\omega t + n\varphi)}, \tag{22}$$

where $|\bar{y}_0|$ is the constant amplitude of displacement, and φ is the interblade phase angle IBPA (phase shift) ([19] p. 192). The interblade phase angle introduced in (22) is used in flutter analysis in order to model the movement of the blades of the palisade.

The aerodynamic force of the considered airfoil is defined from the expression:

$$L_A = \left(\frac{\rho V^2 bh}{2} |\bar{y}_0| \sum_{n=-2}^{2} l_{ny} e^{jn\varphi} \right) \cdot e^{j\omega t}. \tag{23}$$

Similarly for the angular harmonic displacements of airfoils

$$\alpha_n = |\alpha_0|\, e^{j(\omega t + n\varphi)} \tag{24}$$

The aerodynamic moment M_A of the considered airfoil could be obtained from the expression:

$$M_A = \left(\frac{\rho V^2 b^2 h}{2} |\alpha_0| \sum_{n=-2}^{2} m_{n\alpha} e^{jn\varphi} \right) \cdot e^{j\omega t}. \tag{25}$$

The aeroelastic behavior of the system "flow-cascade" without taking into account the mechanical damping is defined by the aerodynamic work which is equal to the work performed by aerodynamic forces during one cycle of oscillations:

$$W_M = \int_0^{\frac{2\pi}{\omega}} M_A \frac{d\alpha}{dt}\, dt \tag{26}$$

for torsional oscillations, and

$$W_L = \int_0^{\frac{2\pi}{\omega}} L_A \cdot \frac{dy_n}{dt}\, dt \tag{27}$$

for bending oscillations. Eqs. (26) and (27) can be written in the form:

$$\begin{aligned} W_M &= \pi \cdot |M_A| \cdot |\alpha_0| \cdot \sin(\phi_M) = \pi \cdot Im\left(\frac{M_A}{e^{j\omega t}}\right) \cdot |\alpha_0| = \pi \frac{\rho V^2 b^2 h}{2} \cdot Im\,(C_m) \cdot |\alpha_0|^2, \\ W_L &= \pi b \cdot |L_A| \cdot |\bar{y}_0| \cdot \sin(\phi_L) = \pi b \cdot Im\left(\frac{L_A}{e^{j\omega t}}\right) \cdot |\bar{y}_0| = \pi \frac{\rho V^2 b^2 h}{2} \cdot Im\,(C_l) \cdot |\bar{y}_0|^2, \end{aligned} \tag{28}$$

where ϕ_M, ϕ_L are the phase angles of the moment and force, $C_m = \sum_{n=-2}^{2} m_{n\alpha} e^{jn\varphi}$, $C_l = \sum_{n=-2}^{2} l_{ny} e^{jn\varphi}$.

The aerodynamic work coefficient can be calculated:

$$Im\,(C_m) = W_M / (\pi \frac{\rho V^2 b^2 h}{2} \cdot \cdot |\alpha_0|^2) \tag{29}$$

$$Im\,(C_l) = W_L \,/ (\, \pi \frac{\rho V^2 b^2 h}{2} \cdot |\bar{y}_0|^2)$$

6 Numerical results

The experimental results were obtained for bending and torsional cascade vibrations, for different interblade phase angles, Strouhal numbers, and the incidence angles respectively.

The geometric parameters of the investigated airfoils cascade are presented in Tabs. 1, 2 and 3. The dimensions of the airfoil were measured in the coordinate system shown in Fig. 7. The angle α_k between chord and tangent to midline of airfoil tip is equal to 2, 86° (see Fig. 5).

Table 1. Geometric paremeters of considered airfoil cascade

blade length	h	0.069 m
chord length	b	0.050 m
circular arc camber		10°
thickness-to-chord ratio		0.07
stagger angle	γ	60°
pitch-to-chord ratio	t/b	0.78
inflow angle	β_1	$(62.86 + i)°$
incidence angle	i	-5, 0, 5, 10, 16
inlet Mach number	M_1	0.16; 0.41
outflow angle	β_2	53°
outflow Mach number	M_2	0.12 ; 0.35
vibration frequency	ν	85.85 Hz
reduced frequency	$Sh\ = (b \cdot 2\pi\nu)\ /\ v_2$	0.616; 0.2
vibration amplitude	$h_0\ \alpha_0$	0.0007 m 0.0084 rad
interblade phase angle	φ	0°, ±45°, ±90°, 180°

Table 2. Coordinates of radius of airfoil edges [mm]

Radius of front edge	0.817
Abscissa of radius of front edge	0.817
Ordinate of radius of front edge	0.879
Radius of tail edge	0.837
Abscissa of radius of tail edge	49.163
Ordinate of radius of tail edge	0.898

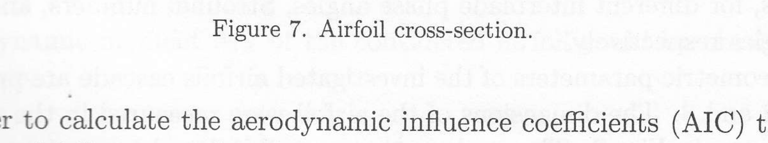

Figure 7. Airfoil cross-section.

In order to calculate the aerodynamic influence coefficients (AIC) the vibrations of the airfoils were induced by turns. The natural frequencies of vibrating system of the experimental test rig are at least 4 times less than the natural fre-

Table 3. Coordinates of suction surface (x_{ss}, y_{ss}) and pressure (x_{pf}, y_{pf}) side of airfoil [mm]

x_{ss}	y_{ss}	x_{pf}	y_{pf}
-3.3	1.047	-3.962	-0.147
1.509	1.698	0.103	0.063
6.298	2.338	4.155	0.264
11.117	2.995	8.241	0.485
15.883	3.621	12.333	0.711
20.458	4.133	16.385	0.913
24.754	4.476	20.352	1.063
28.740	4.635	24.195	1.139
32.448	4.626	27.903	1.134
35.910	4.470	31.504	1.065
39.140	4.174	35.025	0.948
42.149	3.747	38.474	0.787
44.941	3.189	41.848	0.582
47.523	2.505	45.153	0.336
49.940	1.723	48.411	0.061
52.253	0.877	51.646	-0.227

quencies of the cantilever blade. The vibration amplitude of the blade is almost constant along its length and the ratio of amplitudes of the airfoil tip and its root cross section did not exceed 1.033. The experiment was held for excitation frequency $f_r = 85.85$ Hz equal to the natural frequency of the system. The amplitudes of the transitional and angular displacements were assumed as $|\bar{y}_o| = 0.014$ and $|\alpha_o| = 0.0084$ respectively.

The incidence angle i of the experiment was defined as an angle between the tangent to the midline of the blade tip and longitudinal axis, which was parallel to sidewalls of the working section of the wind tunnel. It was based on the assumption that the speed of the incoming flow is parallel to this axis (see Figs. 4 and 5).

To determine parameters of the flow as the density, viscosity, acoustic speed, Mach and Reynolds numbers, the dynamic pressure and static pressure in front of the cascade and the total temperature were measured.

The aerodynamic work coefficients (Eq. (29)) were calculated for different interblade phase angles form 0°, to 360°, the incidence angles from 16° to −5° and different Strouhal number (Figs. 8-21). The calculations were carried out for five determining airfoils ($-2 \leq n \leq 2$).

Figure 8 shows aerodynamic work coefficients as function of the interblade

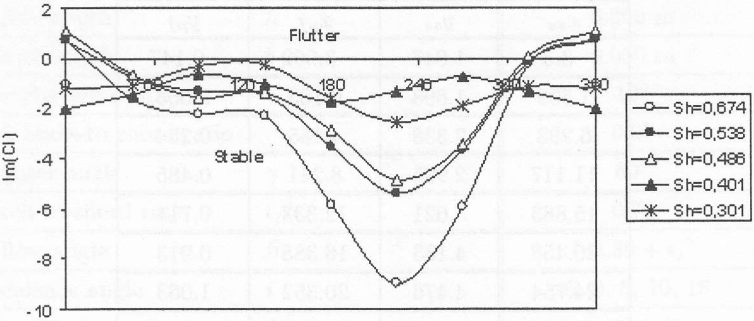

Figure 8. Aerodynamic work coefficient in dependence of IBPA for bending vibration ($i = 16^o$, Strouhal number Sh = 0.301 – 0.674).

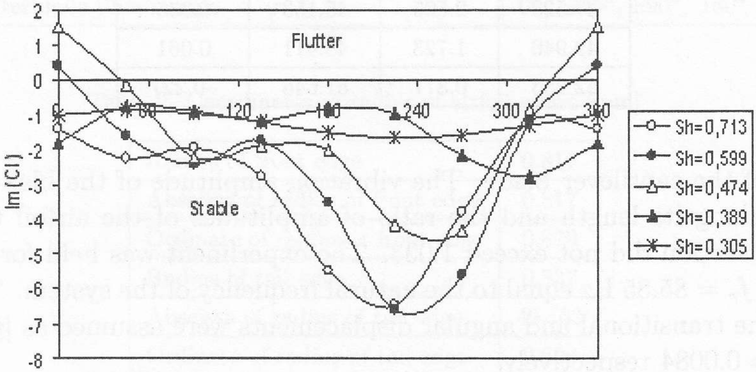

Figure 9. Aerodynamic work coefficient in dependence of IBPA for bending vibration ($i = 14^o$, Strouhal number Sh = 0.305 – 0.713)

phase angle (IBPA) for bending oscillations under incidence flow angle which is equal to 16^o. The negative values of the aerodynamic work coefficients demonstrate the dissipation of oscillating blade energy to the flow (aerodamping), the positive values – to the transfer of the energy from the main flow to the blade (flutter).

The strong influence of both IBPA and Strouhal number on the aerodynamic stability of tune modes is seen in Fig. 8. For Sh = 0.674 the flutter is observed

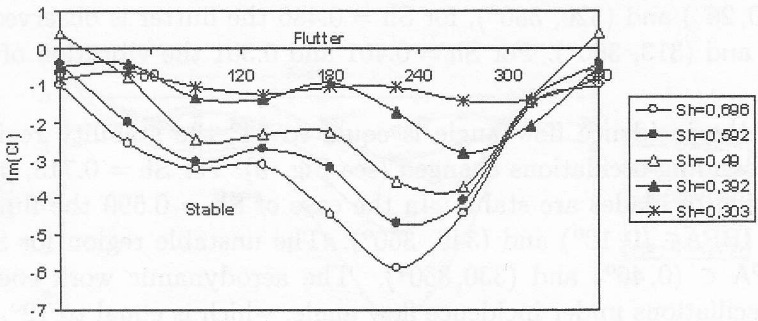

Figure 10. Aerodynamic work coefficient in dependence of IBPA for bending vibration ($i = 12^{\circ}$, Strouhal number Sh = 0.303 − 0.696)

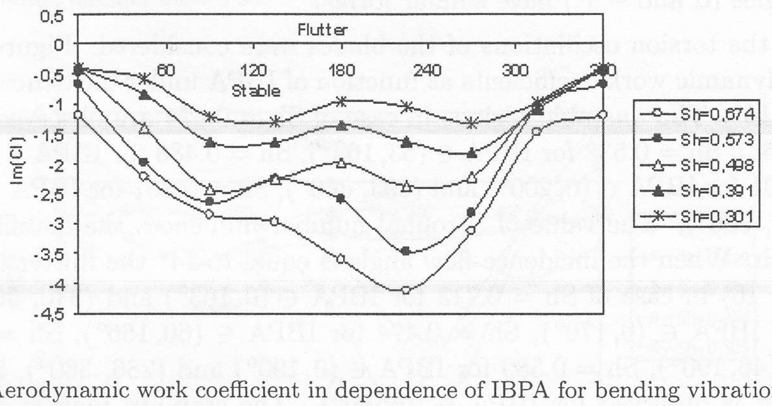

Figure 11. Aerodynamic work coefficient in dependence of IBPA for bending vibration ($i = 10^{\circ}$, Strouhal number Sh = 0.301 − 0.674)

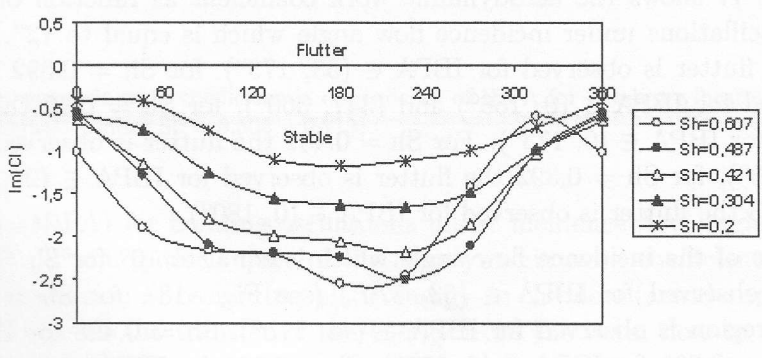

Figure 12. Aerodynamic work coefficient in dependence of IBPA for bending vibration ($i = 5^{\circ}$, Strouhal number Sh = 0.2 − 0.607)

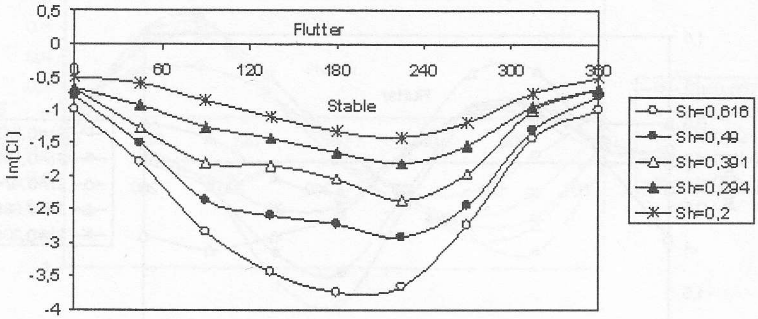

Figure 13. Aerodynamic work coefficient in dependence of IBPA for bending vibration ($i = 0°$, Strouhal number Sh $= 0.2 - 0.616$)

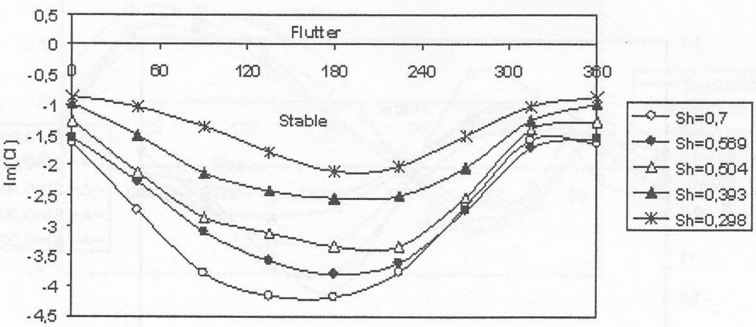

Figure 14. Aerodynamic work coefficient in dependence of IBPA for bending vibration ($i = -5°$, Strouhal number Sh $= 0.298 - 0.7$)

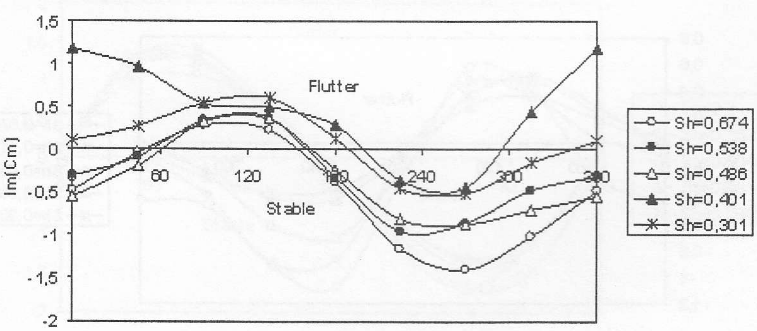

Figure 15. Aerodynamic work coefficient in dependence of IBPA for torsion vibration ($i = 16°$, Strouhal number Sh $= 0.301 - 0.674$)

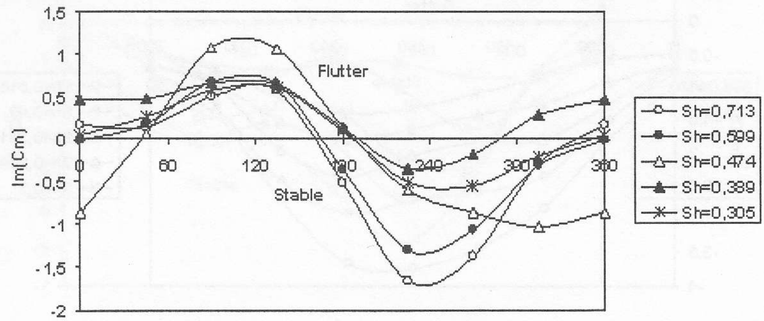

Figure 16. Aerodynamic work coefficient in dependence of IBPA for torsion vibration ($i = 14°$, Strouhal number Sh $= 0.305 - 0.713$)

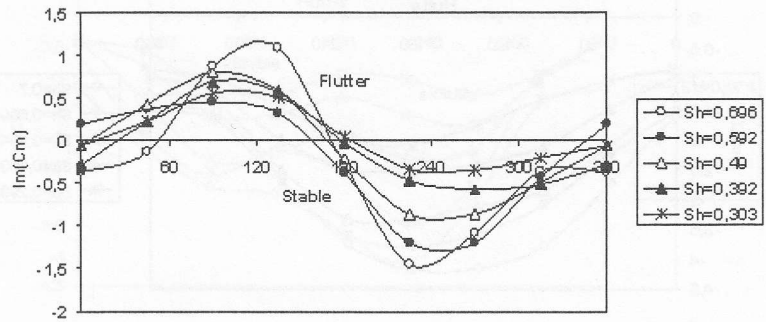

Figure 17. Aerodynamic work coefficient in dependence of IBPA for torsion vibration ($i = 12°$, Strouhal number Sh $= 0.303 - 0.696$)

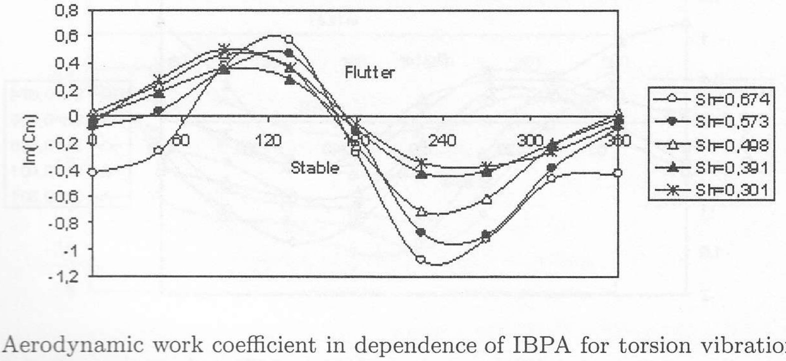

Figure 18. Aerodynamic work coefficient in dependence of IBPA for torsion vibration ($i = 10°$, Strouhal number Sh $= 0.301 - 0.674$)

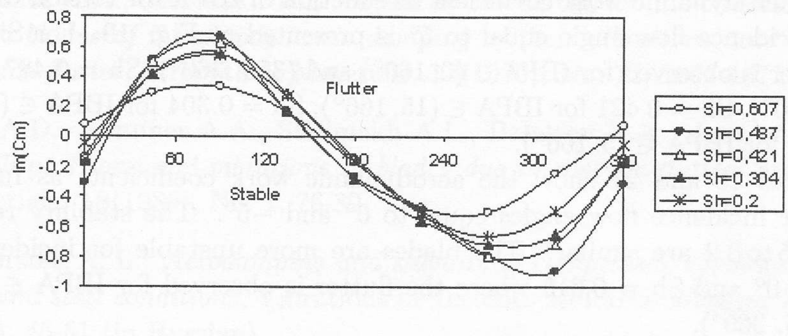

Figure 19. Aerodynamic work coefficient in dependence of IBPA for torsion vibration ($i = 5°$, Strouhal number Sh = 0.2 – 0.607)

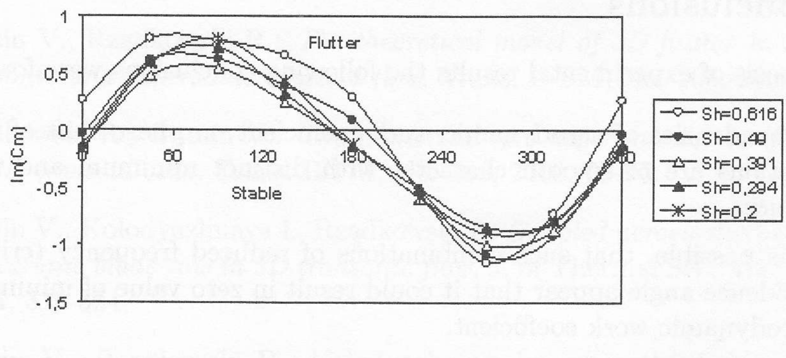

Figure 20. Aerodynamic work coefficient in dependence of IBPA for torsion vibration ($i = 0°$, Strouhal number Sh = 0.2 – 0.616)

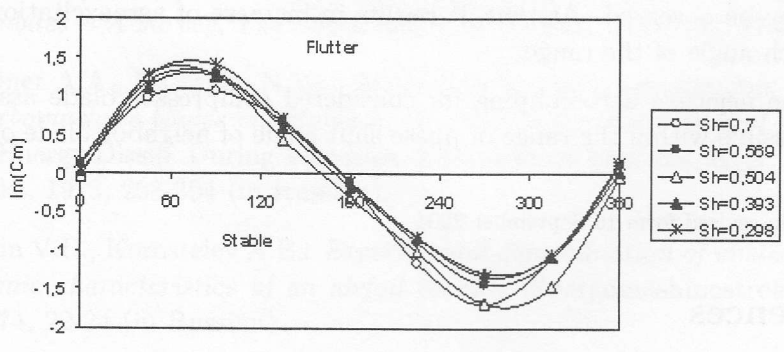

Figure 21. Aerodynamic work coefficient in dependence of IBPA for torsion vibration ($i = -5°$, Strouhal number Sh = 0.298 – 0.7)

The aerodynamic work coefficient as function of IBPA for torsion oscillations under incidence flow angle equal to 5° is presented at Fig. 19. For Sh = 0.607 the flutter is observed for IBPA $\in (0, 160^\circ)$ and $(350, 360^\circ)$, Sh = 0.487 for IBPA $\in (16, 150^\circ)$, Sh = 0.421 for IBPA $\in (15, 166^\circ)$, Sh = 0.304 for IBPA $\in (15, 150^\circ)$, Sh = 0.2 for IBPA $\in (5, 166^\circ)$.

Figures 20 and 21 show the aerodynamic work coefficients as function of IBPA for incidence flow angles equal to 0° and −5°. The stability regions for Sh = 0.5 to 0.2 are similar. The blades are more unstable for incidence angle equal to 0° and Sh = 0.616 where the flutter is observed for IBPA $\in$ (0, 196°) and (345, 360°).

The aerodynamic work coefficient in dependence of IBPA for small incidence flow angle angles (0° and −5°) has a typical sinusoidal form.

7 Conclusions

On the basis of experimental results the following conclusions were formulated:

1. Dependencies of aerodynamic work coefficient on phase shift of blades vibrations are of smooth character with distinct minimum and maximum values;
2. It is possible, that such combinations of reduced frequency (critical) and incidence angle appear that it could result in zero value of minimum blade aerodynamic work coefficient.
3. Independent lowering of reduced frequency value below the critical one, the same as increase of incidence angle, sustaining equality of the others conditions, results in initiation and growth of range of phase shift angles. Within this range negative aerodamping (aeroexcitation) of blades vibration may be observed. At that, it results in increase of aeroexcitation level for each angle of the range.
4. The negative aerodamping for considered compressor blade assemblies is possible within the range of phase shift angle of neighbor blade of $0 \ldots 180^0$

Received in revised form 15 September 2004

References

[1] Stel'makh A.L., Kaminer A.A.: *Effect of the geometrical parameters of a compressor cascade on the limit of bending self-oscillations of blades caused by cascade flutter*, Strength of Materials, **15**(1983), No. 1, 104-109.

[2] Kaminer A.A., Stel'makh A.L.: *Effect of the aerodynamic connectedless between blades of the aerodynamic damping of their vibrations, and origin of cascade flutter*, Strength of Materials, **14**(1996), No. 12, 1667-1672.

[3] Len A.D., Kaminer A.A., Stel'makh A.L., Balalaev V.A.: *Loss of dynamic stability of torsional vibrations of blades due to cascade flutter,* Strength of Materials, **18**(1986), No. 1, 76-80.

[4] Stel'makh A. L.: *Aerodamping and stability of compressor cascades in laminar and stall conditions*, Vibrations in Technics and Technologies, 1999, No. 1(10), 45-51 (in Russian).

[5] A. Bolcs, T.H. Fransson (Eds.): *Aeroelasticity in turbomachines: Comparison of theoretical and experimental cascade results*, Comm. du Labor. de Therm. Appliq. et de Turbomachines, Lausanne, EPFL, N 13, 1986, p. 230.

[6] Gnesin V., Rządkowski R.: *The theoretical model of 3D flutter in subsonic, transonic and supersonic inviscid flow*, Trans. IFFM, No. 106, 2000, 45-68.

[7] Rządkowski R., Gnesin V.: *The numerical and experimantal verification of the 3D inviscid code,* Trans. IFFM, No. 106, 2000, 69-95.

[8] Gnesin V., Kolodyazhnaya L, Rządkowski R: *Coupled aeroelastic oscillations of a turbine blade row in 3D transonic flow*, J. of Thermal Sci., Vol. 10, 2001, No. 4, 318-324.

[9] Gnesin V., Rządkowski R., Kolodyazhnaya L.: *A coupled fluid-structure analysis for 3D flutter in turbomachines*, ASME Paper, No 2000-GT-380, 2000.

[10] Slater J.C., Minkiewicz G.R., Blair A.J.: *Forced response of bladed disk assemblies - A survey*, The Shock and Vibr. Digest, **31**(1999), 17-24.

[11] Caminer A.A., Nastenko N.Ya.: *Method for studying aerodynamic damping of turbomachine blades vibrations in air flows at various modes of vibration*, [in:] Energy Dissip. During Vibration of Mechanical Systems, Kyiv, Naukova Dumka, 1973, 298-304 (in Russian).

[12] Kurzin V.B., Korostelev A.E.: *Experimental determination of unsteady aerodynamic characteristics of an airfoil cascade*, Energomashinostroenye, No. 1, 1974, 22-24 (in Russian).

[13] Karta D., Hiler T.: *The experimental analysis of stability parameters of vibrating cascade in stall transonic flow*, Energetycheske Mashiny i Ustanovky, No. 1(1978), 128-139 (in Russian).

[14] Tanaka H., Fujimoto I., Ishii S.: *Aerodynamic response of a blade in pitching oscillation with partial and full separation*, Novosti Zarubezhnoi Nauki i Tekhniki, 8, 1984, 25-28 (in Russian).

[15] Whitehead D. Watson P. et al.: *The experiment for measurement moment coefficient of the vibrating cascade*, Mir, 1979, 166-177 (in Russian).

[16] Kimura H., Nomiyama A.: *An Experimental Study of Unsteady Aerodynamic Forces an a Rectangular Wing Oscillating in Pitch at Mach Numbers from 0.38 to 1.28*, Memoirs of the Faculty of Eng. Kyushu Univ., 1977, **37**, 3, 157-174.

[17] Kaminer A.A., Chervonenko A.G., Tsymbalyuk V.A.: *Method for studying unsteady aerodynamic characteristics of airfoil cascades vibrating in a three-dimensional flow*, Preprint Inst. for Problems of Strength, Acad. Sci. of the USSR, Kyiv 1988 (in Russian).

[18] Tsimbalyuk V.A.: *Method of measuring transient aerodynamic forces and moments on vibrating cascade*, Strength of Materials, **28**(1996), No. 2, 150-157.

[19] Rządkowski R.: *Dynamics of Rotor Steam Turbine Blading, Part Two, Bladed Discs*, Fluid-Flow Machinery Series, Vol. 22, Ossolineum, Wrocław 1998.